

# Exopolymeric substances of sulfate-reducing bacteria: Interactions with calcium at alkaline pH and implication for formation of carbonate minerals

O. BRAISSANT,<sup>1</sup> A. W. DECHO,<sup>2</sup> C. DUPRAZ,<sup>1,3</sup> C. GLUNK,<sup>3</sup> K. M. PRZEKOP<sup>1</sup> AND P. T. VISSCHER<sup>1</sup>

<sup>1</sup>Center for Integrative Geosciences, University of Connecticut, 354 Mansfield Road, U-2045 Storrs, CT 06269, USA

<sup>2</sup>Arnold School of Public Health, University of South Carolina, 800 Sumter St., Columbia, SC 29208, USA

<sup>3</sup>Institut de Géologie et d'Hydrogéologie, University of Neuchâtel, Rue Emile Argand 158, CH-2009 Neuchâtel, Switzerland

## ABSTRACT

Sulfate-reducing bacteria (SRB) have been recognized as key players in the precipitation of calcium carbonate in lithifying microbial communities. These bacteria increase the alkalinity by reducing sulfate ions, and consuming organic acids. SRB also produce copious amounts of exopolymeric substances (EPS). All of these processes influence the morphology and mineralogy of the carbonate minerals. Interactions of EPS with metals, calcium in particular, are believed to be the main processes through which the extracellular matrix controls the precipitation of the carbonate minerals. SRB exopolymers were purified from lithifying mat and type cultures, and their potential role in CaCO<sub>3</sub> precipitation was determined from acid-base titrations and calcium-binding experiments. Major EPS characteristics were established using infrared spectroscopy and gas chromatography to characterize the chemical functional groups and the sugar monomers composition. Our results demonstrate that all of the three SRB strains tested were able to produce large amounts of EPS. This EPS exhibited three main buffering capacities, which correspond to carboxylic acids (pK<sub>a</sub> = 3.0), sulfur-containing groups (thiols, sulfonic and sulfinic acids – pK<sub>a</sub> = 7.0–7.1) and amino groups (pK<sub>a</sub> = 8.4–9.2). The calcium-binding capacity of these exopolymers in solution at pH 9.0 ranged from 0.12 g<sub>Ca</sub> g<sub>EPS</sub><sup>-1</sup>–0.15 g<sub>Ca</sub> g<sub>EPS</sub><sup>-1</sup>. These results suggest that SRB could play a critical role in the formation of CaCO<sub>3</sub> in lithifying microbial mats. The unusually high sulfur content, which has not been reported for EPS before, indicates a possible strong interaction with iron. In addition to changing the saturation index through metabolic activity, our results imply that SRB affect the rock record through EPS production and its effect on the CaCO<sub>3</sub> precipitation. Furthermore, EPS produced by SRB may account for the incorporation of metals (e.g. Sr, Fe, Mg) associated with carbonate minerals in the rock record.

Received 23 February 2007; accepted 4 July 2007

Corresponding author: O. Braissant, Tel.: +1 860 405 92 40; fax: +1 860 405 91 53; e-mail: Olivier.braissant@uconn.edu

## INTRODUCTION

Seawater is supersaturated with respect to calcium carbonate, but precipitation does not occur spontaneously due to various inhibiting factors. These factors include the high hydration energies of Ca<sup>2+</sup> and Mg<sup>2+</sup> (Slaughter & Hill, 1991), ion-pairing with sulfate, and presence of organic ligands that binds Ca<sup>2+</sup> and Mg<sup>2+</sup> (Wright & Oren, 2005). In lithifying microbial mats (i.e. where calcium carbonate precipitates are found), the metabolic activity of sulfate-reducing bacteria (SRB), which are abundant in mats (Canfield & DesMarais, 1991; Fründ & Cohen, 1992; Visscher *et al.*, 1992), is believed to enhance

calcium carbonate precipitation (Visscher *et al.*, 2000; Dupraz *et al.*, 2004; Baumgartner *et al.*, 2006). The activity of SRB affects the formation of carbonate minerals in several ways. Firstly, sulfate reduction results in a pH increase, affecting the saturation index and thus directly the precipitation of carbonate minerals (Lyons *et al.*, 1984; Walter *et al.*, 1993; Visscher & Stolz, 2005). Secondly, when SRB use low molecular weight organic acids (e.g. lactate, acetate) as electron donors for growth, the availability of free calcium ions may increase due to the removal of carboxylic acids binding calcium (Bosak, 2005; Dupraz & Visscher, 2005). Thirdly, by removing sulfate ions from solution, SRB alter the kinetic

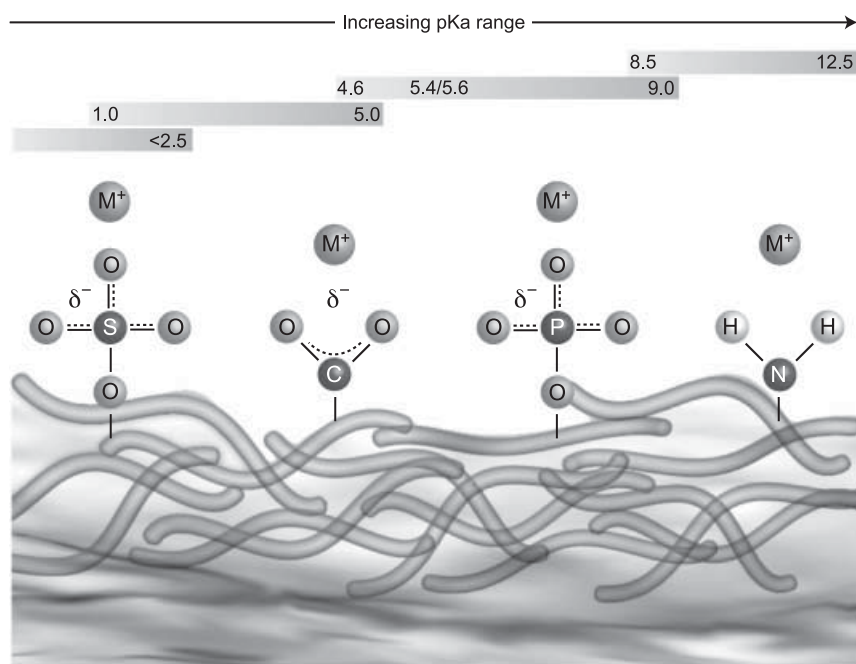


**Fig. 1** Diagram showing the functional groups commonly associated with exopolymeric substances (EPS), and their possible interactions with metals (M<sup>+</sup>). pKa ranges (Stumm & Morgan, 1996; Sokolov *et al.*, 2001) for each functional group are indicated in the upper bar. Note that for phosphoryl groups both pK<sub>1</sub> and pK<sub>2</sub> are considered.

inhibition of dolomite formation (Wright, 1999; Warthmann *et al.*, 2000; van Lith *et al.*, 2003a,b; Wright & Wacey, 2005). Through these processes, the metabolic activity of SRB can be considered as the environmental ‘engine’ that sustains carbonate precipitation in lithifying microbial mats. In addition, the mere presence of SRB cells, even metabolically inactive, may favour calcium carbonate precipitation by providing heterogeneous nucleation sites (Ferris, 2000; Bosak & Newman, 2003).

In a laboratory investigation, *Desulfovibrio* sp., isolated from a corroded surface, chelated metals such as iron, chromium, nickel and molybdenum through production of exopolymeric substances (EPS) (Beech & Cheung, 1995; Zinkevich *et al.*, 1996; Beech *et al.*, 1999). Other studies showed that cyanobacterial EPS was able to bind metal ions such as cadmium, manganese, copper, lead, mercury and calcium to various functional groups that were present in sugars and amino acids constituting the EPS (Somers & Brown, 1978; Mohamed, 2001; Mehta & Gaur, 2007). The negatively charged surface of the cyanobacterial EPS-containing sheath was thought to favour nucleation and precipitation of calcium carbonate (Pentecost, 1985; Riding, 2000). The presence of cyanobacterial EPS also increased the viscosity of the medium, acting as a diffusion barrier, impacting calcium ions mobility, kinetics of precipitation, and consequently the mineralogy of calcium carbonate (Buczynski & Chafetz, 1991). The direct role of cyanobacteria on the CaCO<sub>3</sub> polymorph that precipitated was demonstrated using EPS from *Schizothrix* sp. (Kawaguchi & Decho, 2002). A similar role in carbonate geochemistry could be ascribed to the EPS produced by aerobic heterotrophic bacteria (Hardikar & Matijevic, 2001; Braissant & Verrecchia,

2002; Kim *et al.*, 2005; Lian *et al.*, 2006), and, by extension, probably other groups of bacteria present in biofilms and microbialites (Dupraz & Visscher, 2005).

In lithifying microbial mats, the precipitation of carbonate minerals takes place in an EPS-rich matrix (Dupraz *et al.*, 2004), and remnants of this EPS may be preserved in the rock record (Barbieri & Cavalazzi, 2005; Altermann *et al.*, 2006; Benzerara *et al.*, 2006). The EPS characteristics control the type and quantity of the calcium carbonate minerals produced (Kawaguchi & Decho, 2002; Braissant *et al.*, 2003). Degradation of EPS-containing sheath material was associated with dolomite formation (Wright & Altermann, 2004). The interactions between the metal ions and the EPS are mediated by several functional groups (i.e. specific groups of atoms such as carboxylic acids or amino groups) present in the EPS matrix. Deprotonation of functional groups takes place when the pH increases, providing a negative charge to the polymer (Somers & Brown, 1978; Cox *et al.*, 1999; Socrates, 2001; Phoenix *et al.*, 2002; Fig. 1). In addition to sugar monomers, the EPS matrix may include noncarbohydrate acidic moieties such as pyruvate, succinate, and functional groups such as sulfate or phosphate (Sutherland, 2001a,b,c,d), which also contribute to the overall negative charge of the EPS.

The geochemical role of SRB metabolism in the precipitation of CaCO<sub>3</sub> has been well documented in lithifying mats (Visscher *et al.*, 1992; Reid *et al.*, 2000). Previous work has shown that uncharacterized EPS produced by *Desulfovibrio desulfuricans* G20, isolated from an oil well corrosion site, altered the CaCO<sub>3</sub> mineral morphology (Bosak & Newman, 2005). This important geomicrobiological attribute of SRB has not been assessed in cultures obtained from microbial

mat. Here, we present data that supports the Bosak & Newman (2005) hypothesis that EPS produced by SRB influence the mechanisms of calcium carbonate precipitation. We tested three SRB strains, including isolates from a modern marine stromatolite and a lithifying hypersaline mat, for EPS production. The acid-base properties and the calcium-binding capacity of this EPS were determined to investigate the effects of functional groups on mechanisms of calcium carbonate precipitation.

## MATERIALS AND METHODS

### Bacteria and culture conditions

Three strains of EPS-producing sulfate reducers were used in this study. Strains belonging to the genus *Desulfovibrio* were isolated from a stromatolite surface (Highborne Cay, Bahamas; 76°51'W; 24°42'N): strain: H0407\_12.1Lac; GenBank accession number: DQ822785) and from a microbial mat (Salt Pan, Eleuthera, Bahamas; 76°34'W; 25°24'N); strain LM1, respectively (Baumgartner *et al.*, 2006). The third strain was *Desulfobacterium autotrophicum* (Bak & Widdel, 1986; Brysch *et al.*, 1987), a well-known marine type strain, kindly provided by Dr Leadbetter.

The bacteria were cultured in modified Bak & Widdel (1986) medium, consisting of:  $\text{KH}_2\text{PO}_4$  0.2 g L<sup>-1</sup>,  $\text{NH}_4\text{Cl}$  0.25 g L<sup>-1</sup>,  $\text{KCl}$  0.5 g L<sup>-1</sup>,  $\text{CaCl}_2 \cdot 2\text{H}_2\text{O}$  0.15 g L<sup>-1</sup>,  $\text{MgCl}_2 \cdot 6\text{H}_2\text{O}$  3.0 g L<sup>-1</sup>,  $\text{NaCl}$  20 g L<sup>-1</sup> (except for strain LM1, which was grown with 60 g NaCl L<sup>-1</sup>), and 10 mM  $\text{Na}_2\text{SO}_4$ . After autoclaving and cooling to 60 °C, the following solutions were added: selenite-tungstate solution 1 mL L<sup>-1</sup> ( $\text{NaOH}$  0.5 g L<sup>-1</sup>,  $\text{Na}_2\text{SeO}_3 \cdot 5\text{H}_2\text{O}$  6 mg L<sup>-1</sup>,  $\text{Na}_2\text{WO}_4 \cdot 2\text{H}_2\text{O}$  8 mg L<sup>-1</sup>), mixed vitamins solution 1 mL L<sup>-1</sup> (4-aminobenzoic acid 40 mg L<sup>-1</sup>, D(+)-biotin 10 mg L<sup>-1</sup>, nicotinic acid 100 mg L<sup>-1</sup>, Ca-D(+)-pantothenate 50 mg L<sup>-1</sup>, pyridoxine-2HCl 150 mg L<sup>-1</sup>, thiamine-2HCl 100 mg L<sup>-1</sup>), vitamin B<sub>12</sub> solution 1 mL L<sup>-1</sup> (cyanocobalamin 50 mg L<sup>-1</sup>), SL10 trace element solution ( $\text{FeSO}_4 \cdot 7\text{H}_2\text{O}$  2.1 mg L<sup>-1</sup>,  $\text{MnCl}_2 \cdot 4\text{H}_2\text{O}$  100 mg L<sup>-1</sup>,  $\text{CoCl}_2 \cdot 6\text{H}_2\text{O}$  190 mg L<sup>-1</sup>,  $\text{ZnSO}_4 \cdot 7\text{H}_2\text{O}$  144 mg L<sup>-1</sup>,  $\text{H}_3\text{BO}_3$  6 mg L<sup>-1</sup>,  $\text{NiCl}_2 \cdot 6\text{H}_2\text{O}$  24 mg L<sup>-1</sup>,  $\text{CuCl}_2 \cdot 2\text{H}_2\text{O}$  2 mg L<sup>-1</sup>,  $\text{NaMoO}_4 \cdot 2\text{H}_2\text{O}$  36 mg L<sup>-1</sup>,  $\text{HCl}$  37% 8 mL L<sup>-1</sup>), and 0.1% resazurin solution 0.5 mL L<sup>-1</sup>. Finally, the medium was cooled under  $\text{N}_2/\text{CO}_2$  (80%/20%) flow and 30 mL L<sup>-1</sup> of a 1 M  $\text{NaHCO}_3$  solution (30 mM final concentration), 8 mL of a 0.2 M  $\text{Na}_2\text{S}$  solution (1.6 mM final concentration) to reduce the medium, and 20 mL of a 1 M Na-lactate solution (20 mM final concentration) were added.

Growth of cultures was monitored by measuring the optical density at 600 nm spectrophotometrically (using a Varian Model Cary 50; Varian Inc., Palo Alto, CA, USA). The protein content of the cells was measured using the bicinchoninic acid assay (BCA, Sigma, St. Louis, MO, USA; Smith *et al.*, 1985) with bovine serum albumin (BSA) as standard. The carbohydrate content of the culture was estimated using the phenol-sulfuric acid assay (Dubois *et al.*, 1956). The EPS

content was assayed using Alcian Blue 8GX (Acros Organics, Geel, Belgium) (Passow & Alldredge, 1995; Bober *et al.*, 2005). In this assay, 6 mL of cold ethanol was added to 2 mL of culture sample to precipitate EPS. The sample was then centrifuged for 20 min and the supernatant was discarded. The tube containing the EPS pellet was allowed to air dry for 1 h and after which 2 mL of 0.15 mg mL<sup>-1</sup> Alcian Blue 8GX in 5% acetic acid was added. The mixture was allowed to react for 1 h, after which the absorbance was read at 614 nm. Xanthan was used as a standard. In addition to this assay, EPS dry weight was measured at the end of the culture growth.

### EPS extraction and purification

Exopolymeric substances of SRB were recovered in the early stationary growth phase. Under these conditions, acid-base and calcium-binding properties of the EPS were shown to be consistent in replicate experiments. The culture was prefiltered twice through a glass fibre filter (Whatman GF/F, Whatman Inc., Florham Park, NJ, USA) followed by a single filtration through a 0.2 µm nitrocellulose filter (Sartorius Corp., Edgewood, NY, USA). The EPS in the filtrate was precipitated by adding cold ethanol (4 °C) in a 1 : 1 ratio. Precipitation was allowed to take place for at least 3 h at 4 °C. The EPS was recovered by centrifugation, placed in dialysis tubing (10–12 kDa) and dialysed against de-ionized water (>18 MΩ). After dialysis, the EPS was stored at 4 °C or freeze dried.

### Acid-base titration

The acid-base titration was used to determine the proton-binding sites and gain insight into potential types and densities of the functional groups present in the EPS. For the acid base titration, 2–3 mL of the dialysed EPS (approximately 6.5 mg of dry EPS) was dissolved in de-ionized water (>18 MΩ) to obtain a final volume of 40 mL. The solution was transferred to an anaerobic chamber (COY laboratory product, Grass Lake, MI, USA) under nitrogen (98%) – hydrogen (2%) atmosphere to avoid the formation of carbonate ions due to dissolution of atmospheric  $\text{CO}_2$ . The initial pH of the solution was adjusted to 3.0, which typically required between 100 µL and 150 µL of 1 N HCl, and the solution was titrated with 0.1 N NaOH added stepwise in 10 µL increments. The pH was recorded until pH 11 was reached using an Orion 720 A pH meter (Orion, Boston MA, USA). All reagents were prepared with autoclaved de-ionized water that was allowed to cool to room temperature under vacuum. The titration curves obtained were analysed using the PROTOFIT 2.1 software (Turner & Fein, 2006).

### Calcium titration

The calcium chloride titration was carried out to establish the maximum calcium-binding capacity of the SRB exopolymer. This titration was carried out according to Shimomura &

Inouye (1996) under nitrogen (98%) – hydrogen (2%) atmosphere to avoid the formation of carbonate ions due to dissolution of atmospheric CO<sub>2</sub>. EPS was dissolved in a solution containing 40 mM KCl and 20 mM Tris-OH, which was adjusted to pH 9.0. The titration was carried out by adding a CaCl<sub>2</sub> solution (0.1 or 1 M) in increments of 10 µL to 40 µL to the EPS solution. The concentration of free calcium ions was recorded with a calcium ion-selective electrode (Cole-Palmer Instrument Co., Vernon Hills, IL, USA) and a calomel reference electrode (Fisher Scientific, Waltham, MA, USA) coupled to a high-impedance millivolt meter (Microscale Measurement, The Haag, Netherland). All reagents were prepared using autoclaved de-ionized water that was allowed to cool to room temperature under vacuum. The EPS used for the calcium chloride titration was dialysed 6 h three times each against three different solutions: 1 mM EDTA (pH 8.0), 0.5% acetic acid, and de-ionized water (>18 MΩ).

#### Fourier-transform infrared (FT-IR) spectroscopy of EPS

Fourier-transform infrared spectroscopy (FT-IR) was used in order to determine the presence of specific functional groups such as carboxyl, sulfate, sulfinic acids, thiols, hydroxyl and amino groups of purified EPS (Smith, 1996). EPS was purified by precipitation in ethanol and dialysed as described above. Fresh stromatolite samples were collected on Highborne Cay, Bahamas. Immediately following, natural EPS was extracted and purified as described above for analysis at the University of South Carolina. Analyses were conducted on a Nexus 670 FT-IR Spectrometer (Thermo Nicolet Inc., Waltham, MA, USA) equipped with attenuated total reflectance (ATR) and fitted with a multibounce germanium crystal (Thermo-Nicolet Inc.). Dry EPS samples (approximately 1 mg) were placed in a Thunderdome Tilt-back Pressure Tower (Spectro-Tech Foundation Series, Nicolet, Madison, WI, USA), which is designed to achieve optimal contact between the sample and crystal. This provides an active sampling area of approximately 0.75 mm, with an effective pathlength of 2.03 µm at 1000 cm<sup>-1</sup> (assuming an average index of refraction (for a sample) of 1.5 and an angle of incidence of 45°). Absorbance spectra were collected between 4000 cm<sup>-1</sup> and 600 cm<sup>-1</sup> at a spectral resolution of 4 cm<sup>-1</sup> or 8 cm<sup>-1</sup>, with 32 scans co-added and averaged. If necessary, baseline corrections were carried out. The sulfate content of native EPS was determined by analysing characteristic vibrational peaks near 1160 cm<sup>-1</sup> and 1316 cm<sup>-1</sup>, and quantified using dextran sulfate (Sigma Chem. Co., St. Louis, MO, USA) as a standard (Lijour *et al.*, 1994).

#### Sugar monomer analysis of EPS

The sugar monomer analyses were performed to investigate the monosaccharide composition of the exopolymeric substances of SRB. This monomer composition of intact EPS was measured through glycosyl analyses using chro-

matography combined gas mass spectrometry (GC/MS). Monosaccharide methyl glycosides were prepared by acidic methanolysis and derivatization using per-*O*-trimethylsilyl (TMS) (York *et al.*, 1985; Merkle & Poppe, 1994). Methyl glycosides were prepared from dry samples by methanolysis in 1 M HCl in methanol (80 °C; 18–22 h), followed by re-*N*-acetylation with pyridine and acetic anhydride in methanol for detection of amino acids. Samples were then derivatized (per-*O*-trimethylsilylated) by treatment with Tri-Sil (Pierce Biochemistry, Waltham, MA, USA) at 80 °C for 0.5 h. Myoinositol was added (20 µg to each sample) before derivatization as an internal standard. GC/MS analyses were performed on an HP 5890 GC interfaced to a 5970 MSD (Agilent/HP, Santa Clara, CA, USA) using a Supleco EB1 fused silica capillary column. Monosaccharides were identified by retention times compared to standards, and the carbohydrate character of the peaks was authenticated by their mass spectra. Fragment ion 73 (*m/z*), corresponding to TMS, was used as the characteristic base fragment for all TMS methyl glycosides, 204 and 217 were used to characterize neutral sugars, and 173 was used to characterize amino sugars. Fragment 217 was also used to characterize uronic acids.

## RESULTS

### Cell growth and EPS production

All strains grew and reached the stationary phase (i.e. when cell density monitored as OD<sub>600</sub> levelled off and remained constant; for the cultures in our experiment, this was typically reached at 10<sup>8</sup>–10<sup>9</sup> cells mL<sup>-1</sup>) between 60 and 120 h after inoculation. When comparing the dry weight of EPS produced at the end of cell growth and the results of the Alcian Blue assay and the phenol-sulfuric acid assay, it appeared that only a small fraction of the SRB-EPS was measured by these assays. Nevertheless, assuming that this fraction was constant, the significant correlation between EPS and cell protein indicated that EPS was produced continuously during growth ( $r = 0.96$ ,  $P < 0.05$ , Fig. 2). The EPS and protein concentrations at the end of cultivation were determined for each strain (Table 1) and the sugar monomer composition of the EPS was measured for all three strains (Table 2).

### EPS acid-base titration

The three acid-base titrations performed on EPS extracted from the different sulfate-reducing bacterial strains showed similar patterns, with three main buffering zones (Fig. 3A,B; Table 3). These buffering zones correspond to the capacity of the EPS to counteract the pH changes induced by the addition of NaOH through a release of protons. The first buffering capacity was encountered at a pH close to 3.0 and could be attributed to carboxyl groups (Stumm & Morgan, 1996). Although this buffering capacity was not prominent in the

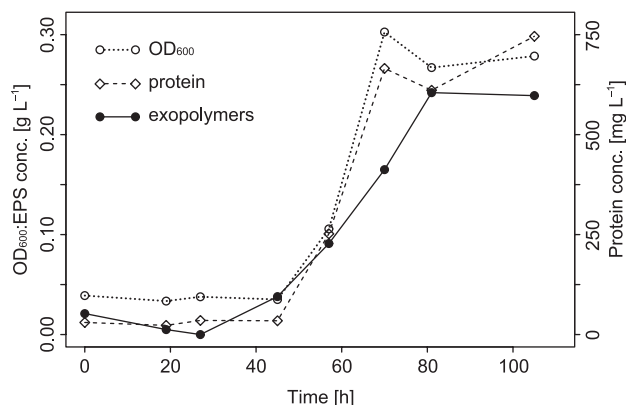


**Fig. 2** Growth of the sulfate-reducing bacteria *Desulfovibrio* sp. (H0407\_12.1Lac), expressed by optical density and protein production. Note the correlation between the protein content and the exopolymer content ( $r^2 = 0.92$ ), suggesting that exopolymers are produced continuously.

**Table 1** Protein, exopolymeric substances (EPS), and the ratio of protein to EPS, produced in the cultures of the different sulfate-reducing bacteria. Cells and EPS were harvested when the early stationary growth phase was reached. EPS was precipitated, freeze-dried and weighed

Strain	Protein [mg L <sup>-1</sup> ]	EPS [mg L <sup>-1</sup> ]	Protein/EPS
<i>Desulfovibacterium autotrophicum</i>	574 ± 18	239 ± 13	2.4
<i>Desulfovibrio</i> sp.*	743 ± 2	239 ± 10	3.1
<i>Desulfovibrio</i> sp.†	235 ± 21	164 ± 6	1.4

\*Strain H0407\_12.1Lac isolated from a stromatolite mat.

†Strain LM1 isolated from a hypersaline lithifying microbial mat.

**Table 2** Analysis of the monomeric sugar composition in the carbohydrate fraction of extracellular polymeric substances (EPS) from different strains of sulfate-reducing bacteria. Values are expressed in mole percentage. Rha, rhamnose; Xyl, xylose; Man, mannose; Gal, galactose; Glc, glucose

	<i>Desulfovibacterium autotrophicum</i>	<i>Desulfovibrio</i> sp.*	<i>Desulfovibrio</i> sp.†
Rha	n.d.	46.2	n.d.
Xyl	28.0	7.2	10.6
Man	15.2	16.2	14.0
Gal	9.0	1.3	19.3
Glc	47.8	29.1	56.1

\*Strain H0407\_12.1Lac isolated from a stromatolite mat.

†Strain LM1 isolated from a lithifying microbial mat.

**Table 3** Apparent pK values observed in the acid-base titration of exopolymeric substances isolated from SRB cultures during early stationary phase

Strain	pK <sub>1</sub>	pK <sub>2</sub>	pK <sub>3</sub>
<i>Desulfovibacterium autotrophicum</i>	3.2 <sup>‡</sup>	7.0	9.2
<i>Desulfovibrio</i> sp.*	3.0 <sup>‡</sup>	7.0	8.7
<i>Desulfovibrio</i> sp.†	3.0 <sup>‡</sup>	6.9	8.5

\*Strain H0407\_12.1Lac isolated from a stromatolite.

†Strain LM1 isolated from a lithifying microbial mat.

‡Lower pK values are expected below the range of the present titration.

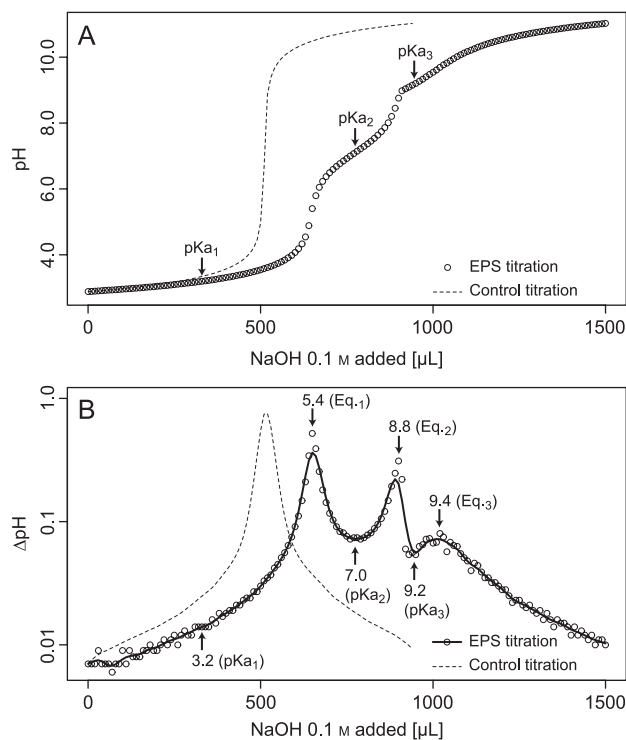


**Fig. 3** (A) Acid-base titration of the exopolymers produced by *Desulfovibacterium autotrophicum* showing three buffering zones (dots). The first zone located around pH 3.2 and below is attributed to carboxyl groups. The second zone located at pH 7.0 is attributed to thiol groups. The third buffering zone at 9.2 is attributed to amino groups. Note that the carboxyl-buffering region can be determined by comparison with the control titration (dashed line). Control titration has been performed using the same volume of deionized water adjusted to the same initial pH with HCl 1 N. (B) Derivative of the acid-base titration curve showing the equivalence points and the apparent pKs values for this exopolymer (dots). Peaks indicate a maximum variation in pH corresponding to the equivalence points and local minima indicate a minimum variation in pH, which is indicative of buffering. Local minima may not appear at the beginning and end of the titration curve due to the small variation in pH. Arrows indicate the corresponding pH value of the titration curve for each equivalence points (Eq.<sub>n</sub>) and half-titration points (i.e. pKs - pKa<sub>n</sub>). Solid line represents a bicubic interpolation used to smooth the data.

derivative of the titration curve (Fig. 3B), comparison with the control revealed a clear difference between the two curves (Fig. 3A). This particular area of buffering was expected to extend beyond pH 3.0, as typical pK values for carboxylic acids range from 1 to 5 (Stumm & Morgan, 1996). The second buffering zone was located at pH 7.0. In view of the large amount of sulfur reported in the EPS of SRB (Beech & Cheung, 1995), this buffering could be attributed to thiol, sulfinic or sulfonic acid groups (Fig. 3). FT-IR spectral data (see below) supported this interpretation, and many thiols, sulfinic and sulfonic acid groups of bioorganic molecules have a pK close to 7.0 (Danehy & Noel, 1960; Kreenov *et al.*, 1960; Stumm & Morgan, 1996). The final buffering zone appeared between pH 8.5 and 9.2. Usually this buffering capacity has been attributed to amino groups (Phoenix *et al.*,

**Table 4** Exopolymeric substances (EPS) pKa values calculated from the EPS acid-base titration curve using PROTOFIT (Turner & Fein, 2006), assuming three binding sites

Strain	pK <sub>1</sub> /SD <sub>pK1</sub>	pK <sub>2</sub> /SD <sub>pK2</sub>	pK <sub>3</sub> /SD <sub>pK3</sub>
<i>Desulfobacterium autotrophicum</i>	2.51 ± 0.08/2.45 ± 0.05	7.03 ± 0.04/1.52 ± 0.01	9.41 ± 0.04/1.52 ± 0.03
<i>Desulfovibrio</i> sp.*	2.62 ± 0.03/2.41 ± 0.08	6.99 ± 0.01/1.70 ± 0.05	8.95 ± 0.01/1.66 ± 0.02
<i>Desulfovibrio</i> sp.†	2.55 ± 0.08/2.46 ± 0.12	6.98 ± 0.01/1.71 ± 0.02	8.80 ± 0.05/1.75 ± 0.03
Functional group	Sulfates	Sulfinic acids	Thiols
	Carboxylic acids	Sulfinic acids, thiols	Amino

\*Strain H0407\_12.1Lac isolated from a stromatolite.

†Strain LM1 isolated from a lithifying microbial mat.

2002). In view of the observed sulfur content of the SRB-EPS in our study, it could be possible that both thiol and amino groups contributed to this third buffering zone. Thiols have a wide range of pKa values (Stumm & Morgan, 1996) including at alkaline pH. Moreover, amino and thiol groups may participate in buffering at higher pH values than investigated here. Similar to our observation for the carboxyl groups, buffering from amino groups was not evident from the derivative of the titration curve, but can be visualized when compared with the titration curve of the control.

Using the PROTOFIT 2.1 software (Turner & Fein, 2006), and assuming three binding sites, the pKa of the proton-binding sites as well as their densities could be estimated (Table 4). Using this software, the first pKa was found between 2.5 and 2.6. There is a slight discrepancy between the fitted values and those observed from the titration curve. A lower pKa range in the fitted data implies that a greater buffering capacity could be expected at low pH values than revealed by the titration. The lower estimated buffering could be attributed to carboxylic acids or to sulfate groups that were present in large amounts in the EPS. Typical pKa values for sulfate groups are usually below 2.5 (Schiewer, 1999). The second fitted buffering zone, between 6.9 and 7.0, corresponding to sulfur compounds (e.g. thiols, sulfinic or sulfonic acids) matched the observed data. The third buffering zone, corresponding to amino groups was estimated by the software between 8.8 and 9.4, is close to the value observed from the titration curve directly. For the three strains, the estimated binding site densities for carboxylic acids, sulfur compounds, and amino groups were estimated to 2.4–2.5 mol kg<sub>EPS</sub><sup>-1</sup>, 1.5–1.7 mol kg<sub>EPS</sub><sup>-1</sup> and 1.5–1.7 mol kg<sub>EPS</sub><sup>-1</sup>, respectively. These observations emphasize the importance of functional groups other than carboxylic acid in the geochemical properties of EPS.

#### Fourier-transform infrared (FT-IR) spectroscopy of EPS

FT-IR analyses (Fig. 4) showed that EPS from *Desulfovibrio* strain H0407\_12.1Lac contained several major infrared absorption peaks. Absorption peaks at 1033 and 1057 cm<sup>-1</sup> were assigned to carbohydrate C-O stretching vibrations. A peak at 1109 cm<sup>-1</sup> could be attributed to S=O, stretching

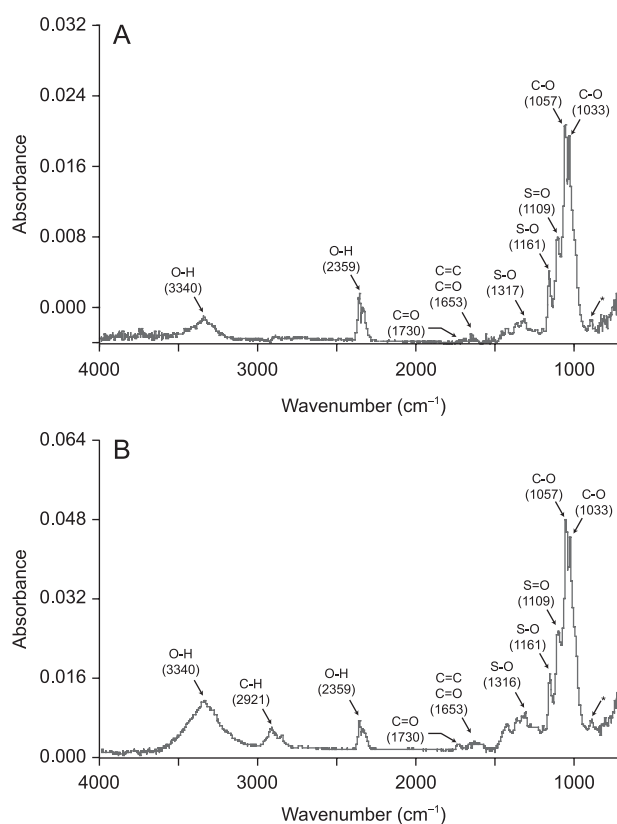


**Fig. 4** FT-IR spectra of purified exopolymeric substances (A) recovered from *Desulfovibrio* sp. (H0407\_12.1Lac) and (B) isolated from a natural stromatolite sample. Asterisk indicates the  $\beta$ -glycoside linkage in polysaccharides.

vibration from sulfinic or sulfonic acid (Coates, 2000; Socrates, 2001). The peak at 1650 cm<sup>-1</sup> was likely due to C=C stretching vibrations, which exist in a vinylidene (i.e. 2H on the same C) conformation (890 cm<sup>-1</sup>). A doublet at 2340 and 2350 cm<sup>-1</sup> could be attributed to the O-H stretching vibrations from sulfinic or sulfonic acids (Coates, 2000; Socrates, 2001). Peaks at 2920 cm<sup>-1</sup> represented C-H stretches, and 3340 cm<sup>-1</sup> represented O-H stretches. Substantial amounts of sulfate were present in EPS derived from SRB isolates, as determined by covalent sulfate peaks at 1161 cm<sup>-1</sup>, representing an S-O stretch accompanied by a deformation

at  $610\text{ cm}^{-1}$ , and a peak at  $1316\text{ cm}^{-1}$ . Although their sugar monomer composition was different (Table 2), the FT-IR spectra for the two other strains (not shown) displayed identical peaks. The sulfate content was estimated at 15–18%, when quantified using dextran sulfate standards. The results of FT-IR analyses also suggested that carboxyl groups could have been present in smaller amounts in these EPS polymers, as they typically form a prominent peak near  $1630\text{--}1650\text{ cm}^{-1}$ , with a shoulder at  $1730\text{ cm}^{-1}$ . Proteins were not detected in the purified EPS by the BCA assay. Therefore, it is unlikely that these peaks could be attributed to amides associated with proteins. Finally, an absorption peak located at  $898\text{ cm}^{-1}$  could be attributed to the  $\beta$ -glycoside linkage between sugar monomers. The major FT-IR peaks in the natural EPS sample were nearly identical to those observed in the pure cultures.

### EPS calcium titration

The titration with calcium chloride revealed that calcium was bound to EPS when compared to the control. At low concentrations of calcium, most was bound or formed complexes and, hence, was not measured by the ion-selective electrode. As the concentration of calcium increased, the available EPS calcium-binding sites were increasingly saturated until no additional calcium was bound. This clearly occurred, as demonstrated by the plateau when plotting bound calcium against calcium added (Fig. 5). The calcium-binding capacity of the EPS was determined using the fitted curve (Fig. 5). Under our experimental conditions, these maximum calcium-binding capacities for *D. autotrophicum* and the *Desulfovibrio* strain H0407\_12.1Lac isolated from a microbial mat were  $0.15\text{ g}_{\text{Ca}}\text{ g}_{\text{EPS}}^{-1}$  and  $0.12\text{ g}_{\text{Ca}}\text{ g}_{\text{EPS}}^{-1}$ , respectively.

### DISCUSSION

The data presented here constitute, to our knowledge, the first report on the acid-base chemical properties and metal (i.e.  $\text{Ca}^{2+}$ )-binding capacity for EPS produced by sulfate-reducing bacteria. While the titration data describe the overall chemical properties of the exopolymeric substances, FT-IR determines the functional groups, which are responsible for the observed specific chemical properties. Many functional groups have similar pKs, and titration only is insufficient for characterizing EPS. This is relevant because of the pivotal role of SRB in many environmental and industrial processes such as biomineralization and corrosion, metal binding, bioremediation and biofouling (Hines *et al.*, 2002; Megonigal *et al.*, 2003).

The results from the acid-base and calcium titrations show that SRB-EPS have a strong potential to exchange protons and calcium ions with the surrounding (micro)-environment. Moreover, the amount of EPS produced in cultures of the three strains tested shows that this extracellular component

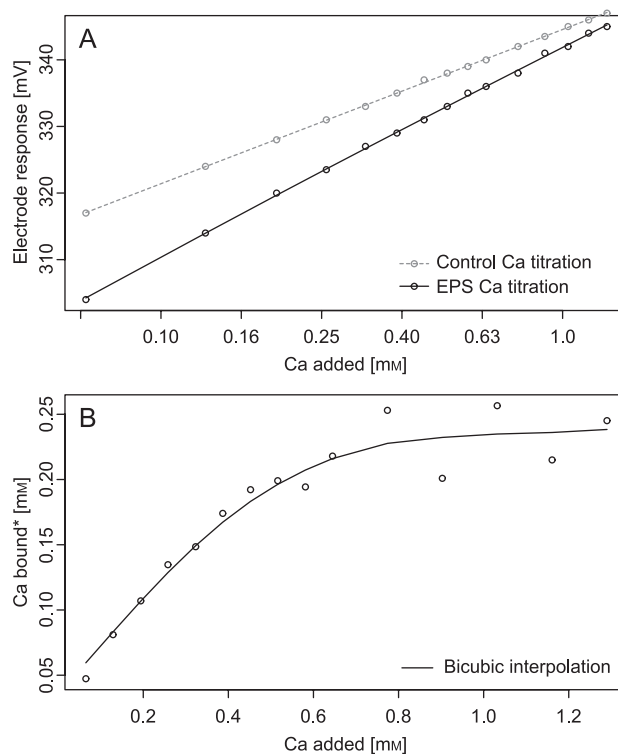
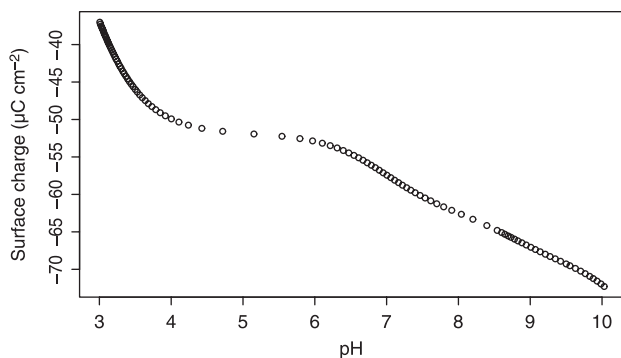


Fig. 5 Calcium chloride titration of *Desulfovibrio autotrophicum* exopolymeric substances (EPS). (A) The calcium electrode response for the control titration (buffer only; dashed line) and for the EPS sample (solid line). (B) Binding capacity of EPS expressed as the calcium bound as a function of the calcium added. (\*Bound calcium is the difference between calcium added and free calcium)

cannot be neglected. Extreme daily fluctuations of the geochemical gradients, especially of pH, are characteristic for natural mats (Visscher *et al.*, 1998; Dupraz *et al.*, 2004). Hence, the different chemical response of the various functional groups constituting the EPS is noteworthy. Carboxylic acid and sulfate groups will always remain deprotonated as pH in the microbial mat will not decrease below pH values of 4.0. This allows the carboxylic acid and the sulfate groups to be efficient metal-binding sites under any typically encountered pH in the lithifying mats. On the contrary, thiol-, sulfonic, sulfonic acid and amino groups with pK values ranging from 7.0 to 9.0 will be subject to periodic changes in protonation states. In other words, these functional groups will not always be able to bind metals, as typical pH in microbial mats may vary from 6.5 to 10.5 (Visscher *et al.*, 1998). However, the functional groups with high pK (i.e.  $\text{pH} > 7.0$ ) values may act as an 'environmental buffer' by initially releasing protons when the pH increases, and similarly, binding protons when the pH decreases. This assists in creating an optimal physiological pH for the SRB and other microbes, and could explain the role of the abundant sulfur groups in the SRB exopolymer. A change in pH from 6.5 to 10.5 will affect the surface charge



**Fig. 6** Surface charge of the exopolymeric substances from *Desulfovibrio* sp. (H0407\_12.1Lac). The surface charge was estimated using the PROTOFIT 2.1 software (Turner & Fein, 2006) and assuming a specific surface area of 416 m<sup>2</sup> g<sup>-1</sup> comparable to agarose (Kuroiwa *et al.*, 2005).

density of the polymer (Fig. 6). In the organomineralization model proposed by Trichet & Défarge (1995), a geometrical change in surface charge induces a template for calcium binding and CaCO<sub>3</sub> nucleation.

The values for calcium binding in this study appear to be high. It is likely that the affinity for calcium is lower in the natural environment due to variations in pH and the presence of competing divalent cations such as magnesium, iron, barium and strontium. Laboratory experiments with xanthan as model EPS show a decrease of the affinity for calcium in the presence of magnesium or strontium (Braissant, 2005). Similarly, data from Disnar & Trichet (1984) demonstrate that copper, cobalt and nickel compete for binding sites in natural exopolymers. However, the binding capacities reported for cadmium (up to 0.43 g<sub>Cd</sub> g<sub>EPS</sub><sup>-1</sup>; Mohamed, 2001) and manganese (up to 0.91 g<sub>Mn</sub> g<sub>EPS</sub><sup>-1</sup>; Mohamed, 2001; Freire-Nordi *et al.*, 2005; Mehta & Gaur, 2007) to cyanobacterial EPS suggest that our Ca-binding values are realistic.

In modern stromatolites and lithifying microbial mats, sulfate-reducing bacteria are closely associated with calcifying aragonitic micritic layers and high-Mg calcite micritic layers (Visscher *et al.*, 2000; Dupraz *et al.*, 2004). The acid-base and Ca-binding properties of SRB-EPS described here will influence the SI of carbonate minerals as well as their morphology and mineralogy. Three main processes characteristic of EPS matrices have been shown to control the precipitation of carbonate minerals: (1) if calcium concentration exceeds the EPS-binding capacity under suitable pH conditions (i.e. pH > 8.4, which value represents the stability of carbonate minerals), precipitation will occur inside the EPS matrix due to local super saturation (Arp *et al.*, 2003); (2) self (re-)arrangement of acidic functional groups in the EPS matrix may create a template that favours the nucleation of carbonate minerals. This process is often referred to as organomineralization (Trichet & Défarge, 1995); and (3) degradation of EPS by heterotrophic bacteria will contribute to the release of calcium,

increasing the SI. Microbial EPS degradation promotes carbonate precipitation by replacing the decaying polymers by (high-Mg) calcite (Dupraz *et al.*, 2004; Decho *et al.*, 2005; Visscher & Stolz, 2005). Many heterotrophic bacteria are known to degrade and grow on various types of EPS (Nankai *et al.*, 1999; Sutherland, 1995, 1999; Hashimoto *et al.*, 1998; Visscher *et al.*, 1999). In this context, release of Ca bound to SRB-EPS is likely to enhance carbonate minerals precipitation. The involvement of SRB-EPS is also supported by the remarkable similarity of FT-IR spectra of EPS extracted from stromatolite mats (Reid *et al.*, 2000) and SRB-EPS (Fig. 5). Such resemblance of EPS from cultures and natural samples suggests that SRB are major contributors to the natural EPS pool, in the stromatolite lithifying layers where high SRB activity is observed. Other organisms such as cyanobacteria also produce large amounts of polymers containing sulfur functional groups and may have a similar influence. Clearly, this requires further investigation.

The high sulfur content of the EPS in our study indicates that both volatile and nonvolatile sulfur-containing degradation products may be produced during decomposition. Interestingly, high levels of sulfonates were found in a number of microbial mats (Visscher *et al.*, 1999), which were thought to represent an important energy and carbon source for anaerobic heterotrophs (Lovley & Coates, 2000). In addition, the presence and flux of a number of volatile sulfur compounds have been measured in a variety of microbial mats (Visscher & van Gemerden, 1991; Visscher *et al.*, 1994, 2003; Taylor & Visscher 1996; Jonkers *et al.*, 1998), which could potentially result from EPS degradation. The source of the large amounts of volatile compounds typically emitted from mats that greatly impacted the Earth's atmosphere (Pilcher, 2003), has been tied to SRB metabolism (Visscher *et al.*, 2003).

Finally, the present study focused on the importance of EPS-calcium interactions. However, in the geological record, calcium carbonate minerals often include traces of other metal cations such as magnesium, iron and strontium. The interaction of EPS with these metals may lead to the formation of ankerite (Ca(Fe,Mg)(CO<sub>3</sub>)<sub>2</sub>) and dolomite (CaMg(CO<sub>3</sub>)<sub>2</sub>), which are common in sedimentary rocks. In addition, previous X-ray photoelectron spectroscopy studies have shown that SRB-EPS has a strong affinity for iron (Beech *et al.*, 1999). The results from the present study suggest that this affinity for iron may be mediated by sulfur groups such as thiols, sulfinic acids or sulfonic acids, all of which have a high affinity for this metal (Ferris, 2000).

## CONCLUSION

This study demonstrated that sulfate-reducing bacteria isolated from lithifying microbial mats were able to produce large amounts of EPS. Investigation of this EPS revealed a buffering capacity, which was sustained by sulfates, carboxylic acids, thiols, sulfinic acids and amino groups. In addition, the

present study showed that this SRB-EPS has a strong calcium-binding capacity. We conclude that, in addition to their role in increasing alkalinity in modern stromatolites and lithifying microbial mats, SRB have the ability to interact with calcium. They can promote or inhibit the formation of carbonate minerals but also create templates enhancing different mineralogies. SRB played an important role during the geochemical evolution of Earth (Canfield *et al.*, 2000; Paytan, 2000). Therefore, the SRB mechanisms that mediate carbonate mineral formation are of great interest for the interpretation of early rock record. The present work documents the role of the SRB's sulfur-rich EPS matrix, and suggests a role of these polymers in the formation of biosignatures, especially (sulfur-rich) kerogen compounds associated with carbonates (Sinninghe Damste *et al.*, 1989).

## ACKNOWLEDGEMENTS

This work was supported by NSF EAR 0221796 and NSF EAR 0331929 attributed to Pieter Visscher and SNF project funding no. 200021.108141 attributed to Christophe Dupraz. Olivier Braissant wishes to thank the Swiss National Fund for the postdoctoral fellowship grant no. PBNEA-110305 that sponsored a visit UCONN, and Eric P. Verrecchia for his support. This is RIBS contribution #39 and #12 of UConn's Center for Integrative Geosciences.

## REFERENCES

- Altermann W, Kazmierczak J, Oren A, Wright DT (2006) Cyanobacterial calcification and its rock-building potential during 3.5 billion years of Earth history. *Geobiology* **4**, 147–166.
- Arp G, Reiner A, Reitner J (2003) Microbialite formation in seawater of increased alkalinity, satonda crater lake, indonesia. *Journal of Sedimentary Research* **73**, 105–127.
- Bak F, Widdel F (1986) Anaerobic degradation of indolic compounds by sulfate-reducing enrichment cultures, and description of *Desulfobacterium indolicum* gen. nov., sp. nov. *Archives of Microbiology* **146**, 170–176.
- Barbieri R, Cavalazzi B (2005) Microbial fabrics from Neogene cold seep carbonates, Northern Apennine, Italy. *Palaeo* **227**, 143–155.
- Baumgartner LK, Reid RP, Dupraz C, Decho AW, Buckley DH, Spear JR, Przekop KM, Visscher PT (2006) Sulfate reducing bacteria in microbial mats: changing paradigms, new discoveries. *Sedimentary Geology* **185**, 131–145.
- Beech IB, Cheung WS (1995) Interactions of exopolymers produced by sulphate-reducing bacteria with metal ions. *International Biodeterioration and Biodegradation* **35**, 59–72.
- Beech IB, Zinkevich V, Tapper R, Gubner R, Avci R (1999) Study of the interaction of sulphate-reducing bacteria exopolymers with iron using X-ray photoelectron spectroscopy and time-of-flight secondary ionisation mass spectrometry. *Journal of Microbiological Methods* **36**, 3–10.
- Benzerara K, Menguy N, Lopez-Garcia P, Yoon TY, Kazmierczak J, Tyliszczak T, Guyot F, Brown GE (2006) Nanoscale detection of organic signatures in carbonate microbialites. *Proceedings of the National Academy of Sciences* **103**, 9440–9445.
- Bober C, Mojica K, Cooney M (2005) Quantification of single-species marine biofilm with alcian blue. *Journal of Young Investigators* **12**, 1–4.
- Bosak T (2005) Laboratory models of microbial biosignatures in carbonate rocks. PhD Thesis, California Institute of Technology, Pasadena, CA, USA, p. 134.
- Bosak T, Newman DK (2003) Microbial nucleation of calcium carbonate in the Precambrian. *Geology* **31**, 577–580.
- Bosak T, Newman DK (2005) Microbial kinetic controls on calcite morphology in supersaturated solutions. *Journal of Sedimentary Research* **75**, 190–199.
- Braissant O (2005) Carbonatogénèse bactérienne liée au cycle biogéochimique oxalate-carbonate. PhD Thesis, Institut de Géologie, University of Neuchâtel, Neuchâtel, p. 131.
- Braissant O, Verrecchia EP (2002) Microbial biscuits of vaterite in Lake Issyk-Kul (Republic of Kyrgyzstan) – Discussion. *Journal of Sedimentary Research* **72**, 944–946.
- Braissant O, Cailleau G, Dupraz C, Verrecchia EP (2003) Bacterially induced mineralization of calcium carbonate in terrestrial environments: the role of exopolysaccharides and amino acids. *Journal of Sedimentary Research* **73**, 485–490.
- Brysch K, Schneider C, Fuchs G, Widdel F (1987) Lithoautotrophic growth of sulfate-reducing bacteria, and description of *Desulfobacterium autotrophicum* gen. nov., sp. nov. *Archives of Microbiology* **148**, 264–274.
- Buczynski C, Chafetz HS (1991) Habit of bacterially induced precipitates of calcium carbonate and the influence of medium viscosity on mineralogy. *Journal of Sedimentary Petrology* **61**, 226–233.
- Canfield DE, DesMarais DJ (1991) Aerobic sulfate reduction in microbial mats. *Science* **251**, 1471–1473.
- Canfield DE, Habicht KS, Thamdrup B (2000) The Archean sulfur cycle and the early history of atmospheric oxygen. *Science* **288**, 658–661.
- Coates J (2000) Interpretation of infrared spectra, a practical approach. In *Encyclopedia of Analytical Chemistry* (ed. Meyers RA). John Wiley and Sons Ltd, Chichester, UK, pp. 10815–10837.
- Cox JS, Smith DS, Warren LA, Ferris FG (1999) Characterizing heterogeneous bacterial surface functional groups using discrete affinity spectra for proton binding. *Environmental Science and Technology* **33**, 4514–4521.
- Danehy JP, Noel CJ (1960) The relative nucleophilic character of several mercaptans toward ethylene oxide. *Journal of the American Chemistry Society* **82**, 2511–2515.
- Decho AW, Visscher PT, Reid RP (2005) Production and cycling of natural microbial exopolymers (EPS) within a marine stromatolite. *Palaeo* **219**, 71–86.
- Disnar JR, Trichet J (1984) The influence of various divalent cations (UO<sub>2</sub><sup>2+</sup>, Cu<sup>2+</sup>, Pb<sup>2+</sup>, Co<sup>2+</sup>, Ni<sup>2+</sup>, Zn<sup>2+</sup>, Mn<sup>2+</sup>) on the thermally induced evolution of organic matter isolated from an algal mat. *Organic geochemistry* **5**, 865–874.
- Dubois M, Gilles KA, Hamilton JK, Rebers PA, Smith F (1956) Colorimetric method for determination of sugars and related substances. *Analytical Chemistry* **28**, 350–356.
- Dupraz C, Visscher PT (2005) Microbial lithification in marine stromatolites and hypersaline mats. *Trends in Microbiology* **13**, 429–438.
- Dupraz C, Visscher PT, Baumgartner LK, Reid RP (2004) Microbe–mineral interactions: early carbonate precipitation in a hypersaline lake (Eleuthera Island, Bahamas). *Sedimentology* **51**, 745–765.
- Ferris FG (2000) Microbe–metal interactions in sediments. In *Microbial Sediments* (eds Riding RE, Awramik SM). Springer-Verlag, Berlin, Germany, pp. 121–126.
- Freire-Nordi CS, Vieira AAH, Nascimento OR (2005) The metal binding capacity of *Anabaena spiroides* extracellular polysaccharide: an EPR study. *Process Biochemistry* **40**, 2215–2224.

- Fründ C, Cohen Y (1992) Diurnal cycles of sulfate reduction under oxic conditions in microbial mats. *Applied and Environmental Microbiology* **58**, 995–998.
- Hardikar VV, Matijevic E (2001) Influence of ionic and nonionic dextrans on the formation of calcium hydroxide and calcium carbonate particles. *Colloids and Surfaces* **186**, 23–31.
- Hashimoto W, Miki H, Tsuchiya N, Nankai H, Murata K (1998) Xanthan lyase of *Bacillus* sp. Strain GL1 liberates pyruvylated mannose from xanthan side chains. *Applied and Environmental Microbiology* **64**, 3765–3768.
- Hines ME, Visscher PT, Devereux D (2002) Sulfur cycling. *Manual of Environmental Microbiology*, 2nd edn (eds Hurst CJ, Crawford RL, Knudsen GR, McInerney MJ, Stetzenbach LD). American Society for Microbiology Press, Washington DC, pp. 427–438.
- Jonkers HM, Koopmans GF, van Gemerden H (1998) Dynamics of dimethyl sulfide in a marine microbial mat. *Microbial Ecology* **36**, 93–100.
- Kawaguchi T, Decho AW (2002) A laboratory investigation of cyanobacterial extracellular polymeric secretions (EPS) in influencing CaCO<sub>3</sub> polymorphism. *Journal of Crystal Growth* **240**, 230–235.
- Kim IW, Robertson R, Zand R (2005) Effects of some nonionic polymeric additives on the crystallization of calcium carbonate. *Crystal Growth and Design* **5**, 513–522.
- Kreenov MM, Harper ET, Duvall RE, Wilgus HS, Ditsch LT (1960) Inductive effects on the acid dissociation constants of mercaptans. *Journal of the American Chemistry Society* **82**, 4899–4902.
- Kuroiwa T, Shoda H, Ichikawa S, Sato S, Mukataka S (2005) Immobilization and stabilization of pullulanase from *Klebsiella pneumoniae* by a multipoint attachment method using activated agar gel supports. *Process Biochemistry* **40**, 2637–2642.
- Lian B, Hu Q, Chen J, Ji J, Teng HH (2006) Carbonate biomineralization induced by soil bacterium *Bacillus megaterium*. *Geochimica et Cosmochimica Acta* **70**, 5522–5535.
- Lijour Y, Gentric E, Deslandes E, Guezennec J (1994) Estimation of the sulfate content of hydrothermal vent bacterial polysaccharides by Fourier-Transform Infrared spectroscopy. *Analytical Biochemistry* **220**, 244–248.
- Lovley DR, Coates JD (2000) Novel forms of anaerobic respiration of environmental relevance. *Current Opinion in Microbiology* **3**, 252–256.
- Lyons WB, Long DT, Hines ME, Gaudette HE, Armstrong PB (1984) Calcification of cyanobacterial mats in Solar Lake, Sinai. *Geology* **12**, 623–626.
- Megonigal JP, Hines ME, Visscher PT (2003) Anaerobic metabolism and production of trace gases. In *Treatise on Geochemistry* (eds Holland HD, Turekian KK). Elsevier, Amsterdam, pp. 317–424.
- Mehta SK, Gaur JP (2007) Use of algae for removing heavy metal ions from wastewater: progress and prospects. *Critical Reviews in Biotechnology* **25**, 113–152.
- Merkle RK, Poppe I (1994) Carbohydrate-composition analysis of glycoconjugate by Gas-Liquid-Chromatography Mass-Spectrometry. *Guide to Technique in Glycobiology Methods in Enzymology* **230**, 1–15.
- Mohamed ZA (2001) Removal of cadmium and manganese by a non-toxic strain of the freshwater cyanobacterium *Gloethece magna*. *Water Research* **35**, 4405–4409.
- Nankai H, Hashimoto W, Miki I, Kawai S, Murata K (1999) Microbial system for polysaccharide depolymerization: enzymatic route for xanthan depolymerization by *Bacillus* sp. Strain GL1. *Applied and Environmental Microbiology* **65**, 2520–2526.
- Passow U, Alldredge AL (1995) A dye-binding assay for the spectrophotometric measurement of transparent exopolymer particles (TEP). *Limnology and Oceanography* **40**, 1326–1335.
- Paytan A (2000) Sulfate clues for the early history of atmospheric oxygen. *Science* **288**, 626–627.
- Pentecost A (1985) Association of cyanobacteria with tufa deposits: identity, enumeration and nature of the sheath material revealed by histochemistry. *Geomicrobiology Journal* **4**, 285–298.
- Phoenix VR, Martinez RE, Konhauser KO, Ferris FG (2002) Characterization and implications of the cell surface reactivity of *Calothrix* sp. strain KC97. *Applied and Environmental Microbiology* **68**, 4827–4834.
- Pilcher CB (2003) Biosignatures of early earths. *Astrobiology* **3**, 471–486.
- Reid RP, Visscher PT, Decho AW, Stolz JF, Bebout BM, Dupraz C, MacIntyre IG, Pearl HW, Pinckney JL, Prufert-Bebout L, Stegge TF, DesMarais DJ (2000) The role of microbes in accretion, lamination and early lithification of modern marine stromatolites. *Nature* **406**, 991–992.
- Riding RE (2000) Microbial carbonate: the geological record of calcified algal mats and biofilms. *Sedimentology* **47** (Suppl. 1), 179–214.
- Schiewer S (1999) Modelling complexation and electrostatic attraction in heavy metal biosorption by sargassum biomass. *Journal of Applied Phycology* **11**, 79–87.
- Shimomura O, Inouye S (1996) Titration of recombinant aequorin with calcium chloride. *Biochemical and Biophysical Research Communications* **221**, 77–81.
- Sinninghe Damste JS, Eglinton TI, De Leeuw JW, Schenck PA (1989) Organic sulfur in macromolecular sedimentary organic matter. I: structure and origin of sulfur-containing moieties in kerogen, asphaltenes and coal as revealed by flash pyrolysis. *Geochimica Cosmochimica Acta* **53**, 873–889.
- Slaughter M, Hill RJ (1991) The influence of organic matter in organogenic dolomitization: perspective. *Journal of Sedimentary Petrology* **61**, 296–303.
- Smith BC (1996) Fundamentals of Fourier Transform Infrared Spectroscopy. CRC Press, Boca Raton, Florida, p. 202.
- Smith PK, Krohn RI, Hermanson GT, Mallia AK, Gartner FH, Provenzano MD, Fujimoto EK, Goecke NM, Olson BJ, Klenk DC (1985) Measurement of protein using bicinchoninic acid. *Analytical Biochemistry* **150**, 76–85.
- Socrates G (2001) *Infrared and Raman Characteristic Group Frequencies: Tables and Charts*. Wiley, New York, p. 366.
- Sokolov I, Smith DS, Henderson GS, Gorby YA, Ferris FG (2001) Cell surface electrochemical heterogeneity of the Fe(III)-reducing bacteria *Shewanella putrefaciens*. *Environmental Science & Technology* **36**, 341–347.
- Somers GF, Brown M (1978) The affinity of trichomes of blue-green algae for calcium ions. *Estuaries* **1**, 17–28.
- Stumm W, Morgan JJ (1996) *Aquatic Chemistry*. John Wiley & Sons, New York, p. 1022.
- Sutherland IA (1995) Polysaccharide lyases. *FEMS Microbiology Reviews* **16**, 323–347.
- Sutherland IA (1999) Polysaccharases for microbial exopolysaccharides. *Carbohydrate Polymers* **38**, 319–328.
- Sutherland IA (2001a) Biofilm exopolysaccharides: a strong and sticky framework. *Microbiology* **147**, 3–9.
- Sutherland IA (2001b) Exopolysaccharides in biofilms, flocs and related structures. *Water Science and Technology* **43**, 77–86.
- Sutherland IA (2001c) Microbial polysaccharides from Gram-negative bacteria. *International Dairy Journal* **11**, 663–674.
- Sutherland IA (2001d) The biofilm matrix – an immobilized but dynamic microbial environment. *Trends in Microbiology* **9**, 222–227.

- Taylor BF, Visscher PT (1996) Metabolic pathways involved in DMSP degradation. In *Biology and Environmental Chemistry of DMSP and Related Sulfonium Compounds* (eds Kiene RP, Visscher PT, Keller MD, Kirst GO). Plenum Press, New York, pp. 265–276.
- Trichet J, Défarge C (1995) Non-biologically supported organomineralization. *Bulletin de l'Institut Oceanographique de Monaco (Special Issue)* **14**, 203–226.
- Turner BF, Fein JB (2006) Protokit: a program for determining surface protonation constants from titration data. *Computer and Geosciences* **32**, 1344–1356.
- Van Lith Y, Warthmann R, Vasconcelos C, McKenzie JA (2003a) Sulfate-reducing bacteria induce low-temperature Ca-dolomite and high Mg-calcite formation. *Geobiology* **1**, 71–79.
- Van Lith Y, Warthmann R, Vasconcelos C, McKenzie JA (2003b) Microbial fossilization in carbonate sediments: a results of the bacterial surface involvement in dolomite precipitation. *Sedimentology* **50**, 237–245.
- Visscher PT, van Gemerden H (1991) Production and consumption of dimethyl-sulfoniopropionate in marine microbial mats. *Applied and Environmental Microbiology* **57**, 3237–3242.
- Visscher PT, Kiene RP, Taylor BF (1994) Demethylation and cleavage of dimethyl sulfoniopropionate in marine intertidal sediments. *FEMS Microbiology Ecology* **14**, 179–190.
- Visscher PT, Stolz JF (2005) Microbial mats as bioreactors: populations, processes and products. *Palaeo* **219**, 87–100.
- Visscher PT, Prins RA, van Gemerden H (1992) Rates of sulfate reduction and thiosulfate consumption in a marine microbial mat. *FEMS Microbiology Ecology* **86**, 283–394.
- Visscher PT, Reid RP, Bebout BM, Hoefft SE, Macintyre IG, Thompson JA (1998) Formation of lithified micritic laminae in modern marine stromatolites (Bahamas): the role of sulfur cycling. *American Mineralogist* **83**, 1482–1493.
- Visscher PT, Gritzner RF, Leadbetter ER (1999) Low-molecular-weight sulfonates, a major substrate for sulfate reducers in marine microbial mats. *Applied and Environmental Microbiology* **65**, 3272–3278.
- Visscher PT, Reid RP, Bebout BM (2000) Microscale observations of sulfate reduction: correlation of microbial activity with lithified micritic laminae in modern marine stromatolites. *Geology* **28**, 919–922.
- Visscher PT, Baumgartner LK, Buckley DH, Rogers DR, Hogan ME, Raleigh CD, Turk KA, Des Marais DJ (2003) Dimethyl sulphide and methanethiol formation in microbial mats: potential pathways for biogenic signatures. *Environmental Microbiology* **5**, 296–308.
- Walter LM, Bischof SA, Patterson WP, Lyons TW (1993) Dissolution and recrystallization in modern shelf carbonates: evidence from pore water and solid phase chemistry. *Royal Society of London Philosophical Transactions (A)* **344**, 27–36.
- Warthmann R, van Lith Y, Vasconcelos C, McKenzie JA, Karpoff AM (2000) Bacterially induced dolomite precipitation in anoxic culture experiments. *Geology* **28**, 1091–1094.
- Wright DT (1999) The role of sulfate-reducing bacteria and cyanobacteria in dolomite formation in distal ephemeral lakes of the Coorong region, South Australia. *Sedimentary Geology* **126**, 147–157.
- Wright DT, Altermann W (2004) The role of sulfate reducing bacteria in carbonate formation. In *International Workshop on Geomicrobiology – A Research Area in Progress*. Aarhus, Denmark, 28–31 January.
- Wright DT, Oren A (2005) Nonphotosynthetic bacteria and the formation of carbonates and evaporites through time. *Geomicrobiology Journal* **22**, 27–53.
- Wright DT, Wacey D (2005) Precipitation of dolomite using sulphate-reducing bacteria from the Coorong Region, South Australia: significance and implications. *Sedimentology* **52**, 987–1008.
- York WS, Darvill AG, McNeil M, Stevenson TT, Albersheim P (1985) Isolation and characterization of plant cell walls and cell wall components. *Methods in Enzymology* **118**, 3–40.
- Zinkevich V, Bogdarina I, Kang H, Hill MAW, Tapper R, Beech IB (1996) Characterisation of exopolymers produced by different isolates of marine sulphate-reducing bacteria. *International Biodeterioration and Biodegradation* **5**, 163–172.